


Myoepithelial cell-specific expression of stefin A as a suppressor of early breast cancer invasion

Hendrika M Duivenvoorden¹, Jai Rautela^{1,2,3†,4†}, Laura E Edgington-Mitchell^{1,5†}, Alex Spurling¹, David W Greening¹, Cameron J Nowell⁵, Timothy J Molloy⁶, Elizabeth Robbins⁷, Natasha K Brockwell¹, Cheok Soon Lee^{7–10}, Maoshan Chen¹, Anne Holliday⁷, Cristina I Selinger⁷, Min Hu¹¹, Kara L Britt¹², David A Stroud¹³, Matthew Bogyo¹⁴, Andreas Möller¹⁵, Kornelia Polyak¹¹, Bonnie F Sloane^{16,17}, Sandra A O'Toole^{8,18,19*} and Belinda S Parker^{1*} 

¹ Department of Biochemistry and Genetics, La Trobe Institute for Molecular Science, Melbourne, VIC, Australia

² Sir Peter MacCallum Department of Oncology, University of Melbourne, VIC, Australia

³ The Walter and Eliza Hall Institute of Medical Research, Melbourne, VIC, Australia

⁴ Department of Medical Biology, University of Melbourne, VIC, Australia

⁵ Drug Discovery Biology, Monash Institute of Pharmaceutical Sciences, Monash University, Melbourne, VIC, Australia

⁶ St Vincent's Centre for Applied Medical Research, NSW, Australia

⁷ Department of Tissue Pathology and Diagnostic Oncology, Royal Prince Alfred Hospital, Camperdown, NSW, Australia

⁸ Sydney Medical School, University of Sydney, NSW, Australia

⁹ Cancer Pathology and Cell Biology Laboratory, Ingham Institute for Applied Medical Research, and University of New South Wales, NSW, Australia

¹⁰ Cancer Pathology, Bosch Institute, University of Sydney, NSW, Australia

¹¹ Department of Medical Oncology, Dana-Farber Cancer Institute, Harvard Medical School, Boston, Massachusetts, USA

¹² Peter MacCallum Cancer Centre, Melbourne, VIC, Australia

¹³ Department of Biochemistry and Molecular Biology, Monash Biomedicine Discovery Institute, Monash University, Melbourne, VIC, Australia

¹⁴ Department of Pathology, Stanford University School of Medicine, California, USA

¹⁵ Immunology Department, QIMR Berghofer Medical Research Institute, Brisbane, QLD, Australia

¹⁶ Department of Pharmacology, Wayne State University School of Medicine, Detroit, Michigan, USA

¹⁷ Barbara Ann Karmanos Cancer Institute, Wayne State University School of Medicine, Detroit, Michigan, USA

¹⁸ Garvan Institute of Medical Research, Darlinghurst, NSW, Australia

¹⁹ Australian Clinical Labs, Bella Vista, NSW, Australia

*Correspondence to: Belinda S Parker, LIMS, La Trobe University, Melbourne, VIC 3086, Australia. E-mail: belinda.parker@latrobe.edu.au
Sandra A O'Toole, Garvan Institute of Medical Research, Sydney, NSW 2010, Australia. E-mail: s.otoole@garvan.org.au

†Current affiliation.

Abstract

Mammography screening has increased the detection of early pre-invasive breast cancers, termed ductal carcinoma *in situ* (DCIS), increasing the urgency of identifying molecular regulators of invasion as prognostic markers to predict local relapse. Using the MMTV-PyMT breast cancer model and pharmacological protease inhibitors, we reveal that cysteine cathepsins have important roles in early-stage tumorigenesis. To characterize the cell-specific roles of cathepsins in early invasion, we developed a DCIS-like model, incorporating an immortalized myoepithelial cell line (N1ME) that restrained tumor cell invasion in 3D culture. Using this model, we identified an important myoepithelial-specific function of the cysteine cathepsin inhibitor stefin A in suppressing invasion, whereby targeted stefin A loss in N1ME cells blocked myoepithelial-induced suppression of breast cancer cell invasion. Enhanced invasion observed in 3D cultures with N1ME stefin A-low cells was reliant on cathepsin B activation, as addition of the small molecule inhibitor CA-074 rescued the DCIS-like non-invasive phenotype. Importantly, we confirmed that stefin A was indeed abundant in myoepithelial cells in breast tissue. Use of a 138-patient cohort confirmed that myoepithelial stefin A (cystatin A) is abundant in normal breast ducts and low-grade DCIS but reduced in high-grade DCIS, supporting myoepithelial stefin A as a candidate marker of lower risk of invasive relapse. We have therefore identified myoepithelial cell stefin A as a suppressor of early tumor invasion and a candidate marker to distinguish patients who are at low risk of developing invasive breast cancer, and can therefore be spared further treatment.

Copyright © 2017 Pathological Society of Great Britain and Ireland. Published by John Wiley & Sons, Ltd.

Keywords: myoepithelial cells; stefin A; cystatin A; breast cancer; cysteine cathepsins; 3D culture

Received 4 July 2017; Revised 21 August 2017; Accepted 18 September 2017

No conflicts of interest were declared.

Introduction

Ductal carcinoma *in situ* (DCIS) is a non-invasive breast cancer where malignant cells are confined to the ducts of the mammary gland [1]. Due to the recent increase in mammographic screening, between 15% and 25% of newly diagnosed breast cancers in the US are pure DCIS (reviewed in ref [2]). Patients diagnosed with DCIS have an excellent overall survival rate of 98–99% and a risk of local recurrence of ~10–20% at 10 years [2,3]. Breast-conserving surgery along with radiotherapy is a common treatment option for DCIS patients, and although five randomized trials found that radiotherapy reduced local recurrence rates by up to 50%, it did not appear to impact overall survival (reviewed in ref [2]). This highlights the need for markers that predict a good prognosis and those patients who can be spared adjuvant therapies.

Invasive breast cancer occurs when cancer cells break through the boundary of the duct, comprising myoepithelial cells and the basement membrane, and the presence of these features distinguishes DCIS from invasive breast cancer [1,4]. Myoepithelial cells are spindle-shaped cells involved in the deposition of the basement membrane and form a single layer separating the inner layer of luminal epithelial cells from the interstitial stroma [5–7]. They are hypothesized to be natural tumor suppressors that resist malignant tumor transformation, as supported by their ability to suppress tumor growth and invasion *in vitro* and *in vivo* [4,8,9]. Further, myoepithelial cells exhibit a proteinase inhibitor-dominated phenotype [8] that contributes to tumor suppression via the inhibition of proteases that have multiple pro-tumorigenic functions including invasion and angiogenesis [10]. The interaction between tumor and myoepithelial proteases and inhibitors is not well understood, partly due to the lack of models that recapitulate this interaction.

A class of proteases prominently linked to tumorigenesis is the cathepsins, divided into serine, cysteine, and aspartyl types. There are currently 11 identified human cysteine cathepsins: B, H, L, S, C, K, O, F, V, W, and X/Z [11]. These proteases are predominantly lysosomal in normal cells (with functions including autophagy, apoptosis, and antigen presentation [11]), yet commonly detected at the cell surface and secreted in cancer [12], where their expression in tumor and stromal cells has numerous pro-tumorigenic functions including degradation of ECM proteins and promoting angiogenesis and epithelial–mesenchymal transition (EMT) [12–18]. Of the cysteine cathepsins, cathepsin B has been widely implicated in tumor progression and metastasis, including in the MMTV-PyMT breast cancer model [14,19,20]. The cysteine cathepsins (referred to as cathepsins henceforth) are inhibited by their endogenous inhibitors, including the cystatin superfamily, comprising stefin A, stefin B, and cystatin C [21], and our group has previously linked increased tumor cell expression of stefin A with reduced metastatic propensity, in the

absence of an effect on primary tumor growth [22]. It is evident that the delicate balance between cathepsins and their inhibitors is important in tumorigenesis and metastasis (reviewed in ref [11]).

It is clear that active cathepsins play important roles in tumorigenesis, yet the cell-specific role of cysteine cathepsins and their inhibitors in early breast tumorigenesis is unclear. In this study, we utilize an *in vivo* model along with 3D models developed in the laboratory to investigate the cell-specific contribution of protease inhibitors in the DCIS-to-invasive carcinoma transition. We reveal that stefin A is abundant in myoepithelial cells and that expression of this cathepsin inhibitor is critical for the suppressive function of myoepithelial cells. For the first time, we confirm in patient-derived tissues that the expression of stefin A is highly abundant in myoepithelial cells surrounding normal ductal epithelium and low-grade DCIS lesions, but it is reduced in high-grade and micro-invasive DCIS, supporting myoepithelial stefin A as a candidate myoepithelial-specific tumor suppressor.

Materials and methods

Mouse models

Mouse investigations were performed after approval by the La Trobe University Animal Ethics Committee. BI/6 MMTV-PyMT-positive female mice were injected (intraperitoneally, 200 µl/20 g mouse) daily with 50 mg/kg CA-074 (cathepsin B inhibitor; synthesized and purified in the Bogoy Laboratory, Stanford, CA, USA) or vehicle (5% DMSO/saline) from day 30 to day 49. Following treatment, mammary gland sections were scored by a pathologist blinded to treatment groups (S O'Toole) for the presence of invasive regions of cancer growth within the mammary gland. Experiments included eight mice per group.

Derivation of the N1ME myoepithelial cell line

De-identified fresh human breast reduction mammaplasty tissue was collected using protocols approved by the Institutional Review Board and digested to single cell suspension. Myoepithelial cells were immunopurified using anti-CD10 magnetic beads (CD10 antibody, M0727, 1:80–1:160 dilution; Dako, Santa Clara, CA, USA; Beads, 110.23, Pan mouse IgG; Dynal/Thermo Fisher Scientific, Waltham, MA, USA) as described previously [23]. The retroviral expression vector pMSCV-CMV-puro-hTERT was transfected into Phoenix packaging cells using Eugene6 (Promega, Madison, WI, USA). Conditioned medium was filtered and incubated with the myoepithelial primary cells along with polybrene. Myoepithelial cells were then selected using 0.4 µg/ml puromycin and named N1ME. Initially, the cells were grown in Medium 171 (M-171-500; Cascade Biologics/Thermo Fisher Scientific) supplemented with mammary epithelial

growth supplement (MEGS; Cascade Biologics/Thermo Fisher Scientific; S-015-5), penicillin/streptomycin, and puromycin. Recently, the N1ME cell line has been maintained in Mammary Epithelial Cell Growth Medium (MEGM) (Lonza, Basel, Switzerland; CC3151) with Single Quot supplements (Lonza; CC-4136). After some passaging, the N1ME cell line was retrovirally infected with pMSCV-mCherry vector, as described above but with the PT67 packaging cell line transfected using Lipofectamine (Invitrogen, Carlsbad, CA, USA), and sorted by flow cytometry performed using standard techniques.

Cell culture

The MCF10.DCIS.com (DCIS.com) cell line was derived from the MCF10 model [24] and maintained in DMEM:Nutrient Mix F-12–5% FBS–1% penicillin/streptomycin. The MDA-MB-231, MDA-MB-231-GFP, and CAL-120 cell lines were maintained in DMEM–10% FBS–1% penicillin/streptomycin. All cell lines were maintained at 37 °C, 5% CO₂. Cell line details and TALEN and siRNA constructs used to disrupt expression or knockdown proteins of interest are described in the supplementary material, Supplementary materials and methods. It should be noted that 3D co-cultures using these lines utilized the MEGM media listed above.

FACS analysis

N1ME, DCIS.com, and MDA-MB-231 cells were assessed for basal, luminal, and myoepithelial cell markers as previously described [25]. In brief, cells were stained with a cocktail of lineage markers (PE-conjugated CD45, CD235a, CD31) and then with epithelial subpopulation-specific markers (EpCAM-PB and CD49f-PE-Cy7). All cells were resuspended in propidium iodide to allow gating on viable cells only. The BD LSR Fortessa X20 (Becton Dickinson, Franklin Lakes, NJ, USA) was used to analyze all samples. Compensation was completed manually at the time of sample acquisition, using single-color controls in each experiment. All data files were analyzed using the free software program FlowLogic™ (Miltenyi Biotec, Bergisch Gladbach, Germany)

3D cell culture

All 3D cultures were performed using a reconstituted basement membrane, Cultrex® (3433-005-01; Trevigen, Gaithersburg, MD, USA). Glass-bottom eight-well chambers (NUN155409; Thermo Fisher Scientific) were coated with 100% Cultrex and allowed to solidify at 37 °C for 20 min. Cells (pre-mixed at a predetermined ratio) were seeded on top of the solidified Cultrex and allowed to adhere for 60–90 min before 2% Cultrex in MEGM (used for N1ME culturing, as mentioned above) was overlaid. The medium was changed every 4 days unless otherwise stated. Inhibitor 3D studies were performed by the addition to the medium of 50 µM

of the highly selective cathepsin B inhibitor CA-074 or the pan-cysteine cathepsin inhibitor JPM-OEt (Drug Synthesis and Chemistry Branch, Division of Cancer Treatment and Diagnosis, National Cancer Institute, Bethesda, MD, USA) reconstituted in DMSO, or DMSO as control; this was refreshed every 48 h. Microscopy techniques are described in the supplementary material, Supplementary materials and methods. For quantification, bright field images of 3D cultures were processed and analyzed using the Fiji distribution of ImageJ [26] as described in the supplementary material, Supplementary materials and methods.

Protease labeling and western blotting

The protocol followed was as previously described [27]. Specifically, for cathepsin B activity gels, activity-based probes [GB123 (1 µM) [28] or BMV109 (0.1 µM) [29]] were added to lysates from a 100× stock, and proteins were incubated for 30 min at 37 °C. Antibody details are provided in the supplementary material, Supplementary materials and methods.

Mass spectrometry: isolation, enrichment, and proteomic analysis of N1ME, DCIS.com, and MDA-MB-231 cell lysates

Cell lysates were prepared from human breast N1ME, DCIS.com, and MDA-MB-231 cells (~1 × 10⁶ cells) using detergent cell lysis and centrifugation, as detailed in the supplementary material, Supplementary materials and methods. Cellular lysates were analyzed by mass spectrometry-based proteomics using an in-gel digestion approach followed by nanoliquid chromatography (Ultimate 3000 RSLCnano, Thermo Fisher Scientific) coupled directly to a Q-Exactive HF Orbitrap (Thermo Fisher Scientific) mass spectrometer operated in data-dependent acquisition mode, as described in the supplementary material, Supplementary materials and methods. The mass spectrometry proteomics data have been deposited in the PeptideAtlas repository (<http://www.peptideatlas.org/>) with the data set identifier PASS01048.

Immunohistochemistry (IHC)

For human tissues, normal breast sections and primary breast carcinoma samples were obtained from S O'Toole at the Royal Prince Alfred Hospital (RPAH) either as full-faced slides (for the micro-invasive carcinoma) or in a tissue microarray [30]. The use of archived human tissues was approved by the HREC of RPAH [approval number X15-0388 (SSA/16/RPAH/397)]. Sections (formalin-fixed, paraffin-embedded) were stained with 1 µg/ml anti-human stefin A (1:1000) (ab61223; Abcam, Cambridge, UK), p63 (1:80) (DAK-p63, following antigen retrieval in pH 9 EDTA buffer for 30 min; Dako), anti-human α-smooth muscle actin (1:500) (ab66133; Abcam) or with isotype control antibodies (1:19000), overnight at 4 °C, and detected with a biotin-conjugated secondary antibody (Vector Laboratories, Burlingame,

CA, USA). Human stefin A staining was scored by an independent pathologist, Dr E Robbins (see supplementary material, Supplementary materials and methods).

Statistical analysis

Statistics were conducted using the data analysis software package within GraphPad Prism v7 for Windows (GraphPad Software, La Jolla, CA, USA) and PASW Statistics 18 (SPSS, Chicago, IL, USA). Error bars indicate SEM unless otherwise stated.

Results

Treatment with cathepsin B inhibitors decreases invasive growth *in vivo*

It has been well documented that cysteine cathepsins and their inhibitors have important roles in breast cancer; however, their role in early breast cancer is not well studied. To test the therapeutic efficacy of cathepsin inhibitors in the DCIS-to-invasive carcinoma transition in an *in vivo* model of early tumorigenesis, we treated MMTV-PyMT mice (which spontaneously develop mammary gland tumors [31]) with the cathepsin B-selective inhibitor CA-074 for the time period between DCIS and invasive carcinoma development in this model (30–50 days; supplementary material, Figure S1A). At the time of treatment cessation, mammary glands were histologically evaluated (Figure 1A). Comparison of the control (DMSO) group versus the treatment (CA-074) group revealed that cathepsin B inhibition decreased the number of invasive regions detected in the mammary glands from 6/8 (75%) to 2/8 (25%) mice, respectively (Figure 1B, C). This was independent of tumor cell proliferation, as confirmed by equivalent Ki67 staining in control and treatment groups (supplementary material, Figure S1B). Together, these data supported a functional role for cathepsins in early tumorigenesis and prompted analysis of cell-specific functions.

Characterization of a myoepithelial cell line

The presence of an intact myoepithelial layer is the key distinguishing factor between DCIS and invasive pathologies; hence, to investigate this interaction *in vitro*, we utilized the immortalized N1ME myoepithelial line that was recently described [32]. N1ME cells have smooth muscle cell-like morphology when grown in 2D and grow in spheroids in 3D (supplementary material, Figure S2A, B), as expected. To confirm that N1ME cells expressed basal cell markers, we used flow cytometry to measure the cell surface expression of EpCAM and CD49f, markers previously accepted to distinguish luminal, basal, and stromal populations [25]. The N1ME cells had high CD49f and low EpCAM, characteristic of basal cells (Figure 2A).

This also confirmed a lack of contaminating breast myofibroblasts, which have previously been identified in the EpCAM-low/CD49f-low stromal compartment [25]. As controls, we used DCIS.com and the basal MDA-MB-231 cells which expressed luminal breast progenitor markers (EpCAM high/CD49f⁺) and basal-like markers, respectively (Figure 2A). Further interrogation using mass spectrometry revealed 388 proteins uniquely expressed in N1ME cells in comparison to the DCIS.com and MDA-MB-231 cells (supplementary material, Figure S2C and Table S1). Comparison with protein signatures previously identified for purified normal breast myoepithelial and luminal cells [33] revealed that the N1ME cells indeed expressed myoepithelial markers and lacked the epithelial and tumor cell markers expressed in the DCIS.com and MDA-MB-231 cell lines (Figure 2B and supplementary material, Table S2). Together, these data supported the myoepithelial identity of the N1ME cell line.

Recapitulating DCIS *in vitro* using a 3D co-culture model

We next developed a 3D model incorporating the N1ME cell line and invasive breast tumor cell lines. This line has only been used in culture with the non-invasive DCIS.com line to date [32]. In 3D culture, the invasive triple-negative MDA-MB-231 cells grew in invasive protrusions spreading through the Cultrex (Figure 2C, blue Hoechst-stained). Importantly, co-culture of these cells with N1ME revealed a clear reversion of this invasive phenotype, whereby the addition of N1ME (red) cells reverted growth of this cell line to a DCIS-like phenotype (Figure 2C), which was maintained for over 14 days (supplementary material, Figure S2D). This restriction of invasion by N1ME cells was also observed using the CAL120 triple-negative invasive breast cancer cell line (Figure 2F). This phenotype was specific to myoepithelial cells in 3D culture and could not be recapitulated in 2D culture (supplementary material, Figure S2E) or using non-myoepithelial cell lines (supplementary material, Figure S2F).

To compare statistically the difference in tumor cell invasion when cultured in 3D alone or in combination with N1ME cells, we used a measure of circularity (the perimeter to convex hull ratio; supplementary material, Figure S2G–J). This quantitative measurement revealed that the addition of N1ME myoepithelial cells to invasive cancer cells resulted in more circular colonies, and hence fewer invasive structures in these co-cultures (Figure 2D, E, G, H).

Reduction of stefin A expression promotes breast cancer cell invasion

Given our *in vivo* results implicating cathepsins in early invasion, we investigated the expression of cathepsin B and the cystatin family of cathepsin inhibitors in the tumor and myoepithelial cell lines incorporated

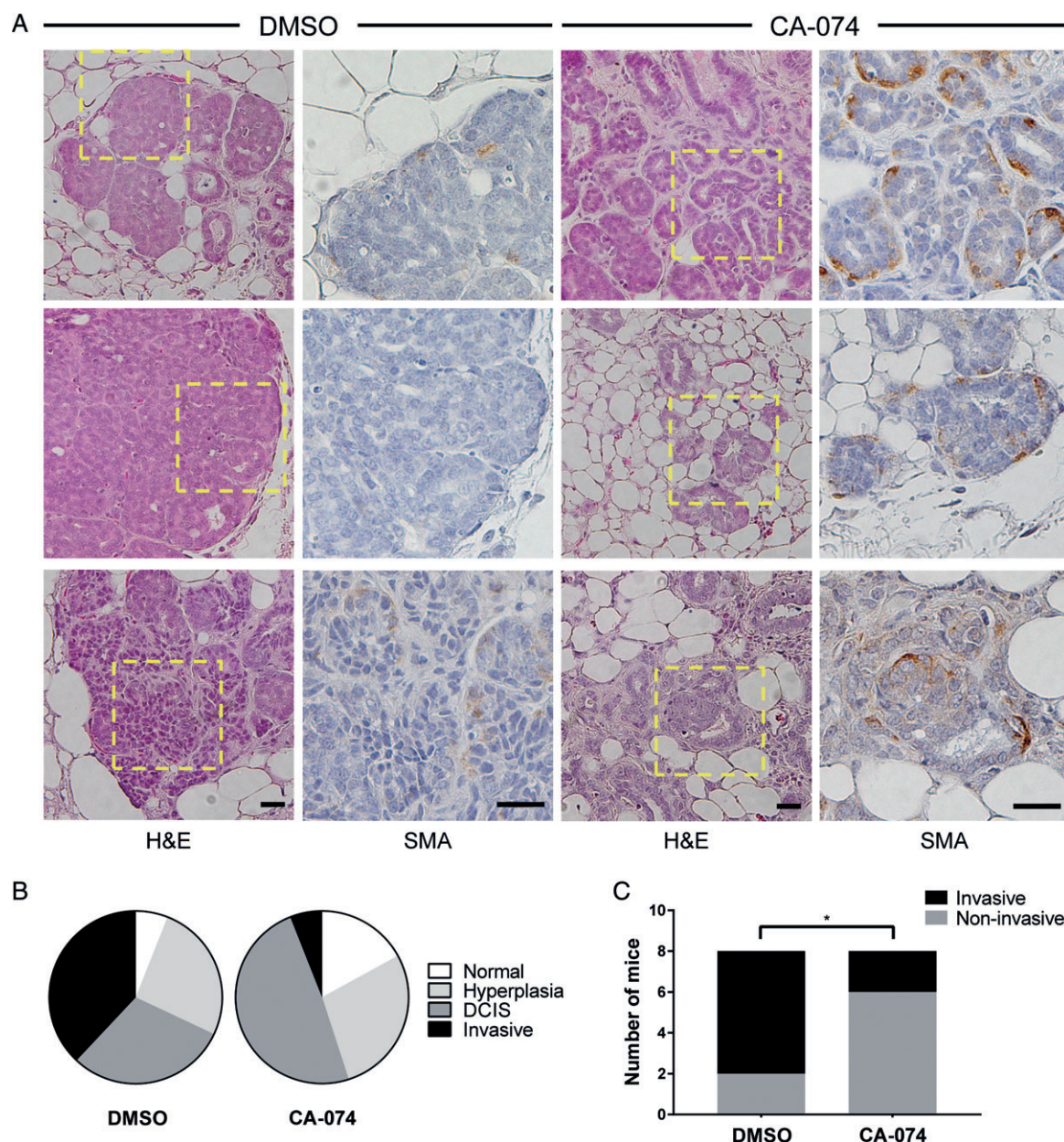


Figure 1. Cysteine cathepsin inhibition *in vivo* decreases the development of invasive lesions in mouse mammary glands. (A) Representative images of second, third or fourth mammary glands with DCIS/invasive regions from mice treated with 50 mg/kg CA-074 or DMSO (control) in saline for 20 days. At day 50, mice were culled and mammary glands harvested, sectioned, and stained by H&E. Serial sections were stained with anti-smooth muscle actin (myoepithelial marker) and visualized with DAB. These sections were counterstained with hematoxylin. Representative images from eight mice per group. Scale bars represent 25 μ m. Mammary glands of all mice were scored by a pathologist without knowledge of the experimental group and were determined to be invasive or non-invasive (normal, hyperplasia, DCIS). (B) Percentage of mammary glands with each diagnosis per group. (C) The final diagnosis for each mouse was determined and compared between groups. * $p < 0.05$ by chi-square test.

in the 3D model. Interestingly, N1ME cells have a cathepsin inhibitor-dominant phenotype, with high levels of stefin A and stefin B detected and to a lesser extent cystatin C (Figure 3A). In tumor cell lines, levels of stefin A were inversely correlated with invasive phenotype, with MDA-MB-231 cells having the lowest expression (Figure 3A). Stefin B was expressed at similar levels in all cell lines, while cystatin C expression was elevated in the more invasive cell lines (MDA-MB-231 and CAL120, Figure 3A). Although the levels of mature (25/30 kDa) and pro (50 kDa) cathepsin

B were similar in all cell lines (Figure 3Bi), use of the activity-based probe GB123 [28] confirmed that cathepsin B activity was increased in the tumor line with the highest metastatic potential (MDA-MB-231, Figure 3Biii), as expected in view of its pro-tumorigenic roles. In contrast, cathepsin L activity did not correlate with metastatic potential or cystatin expression. Importantly, the N1ME cells had very low cathepsin B activity (Figure 3Biii), most likely due to inhibition by the cystatins, which are abundantly expressed in these cells.

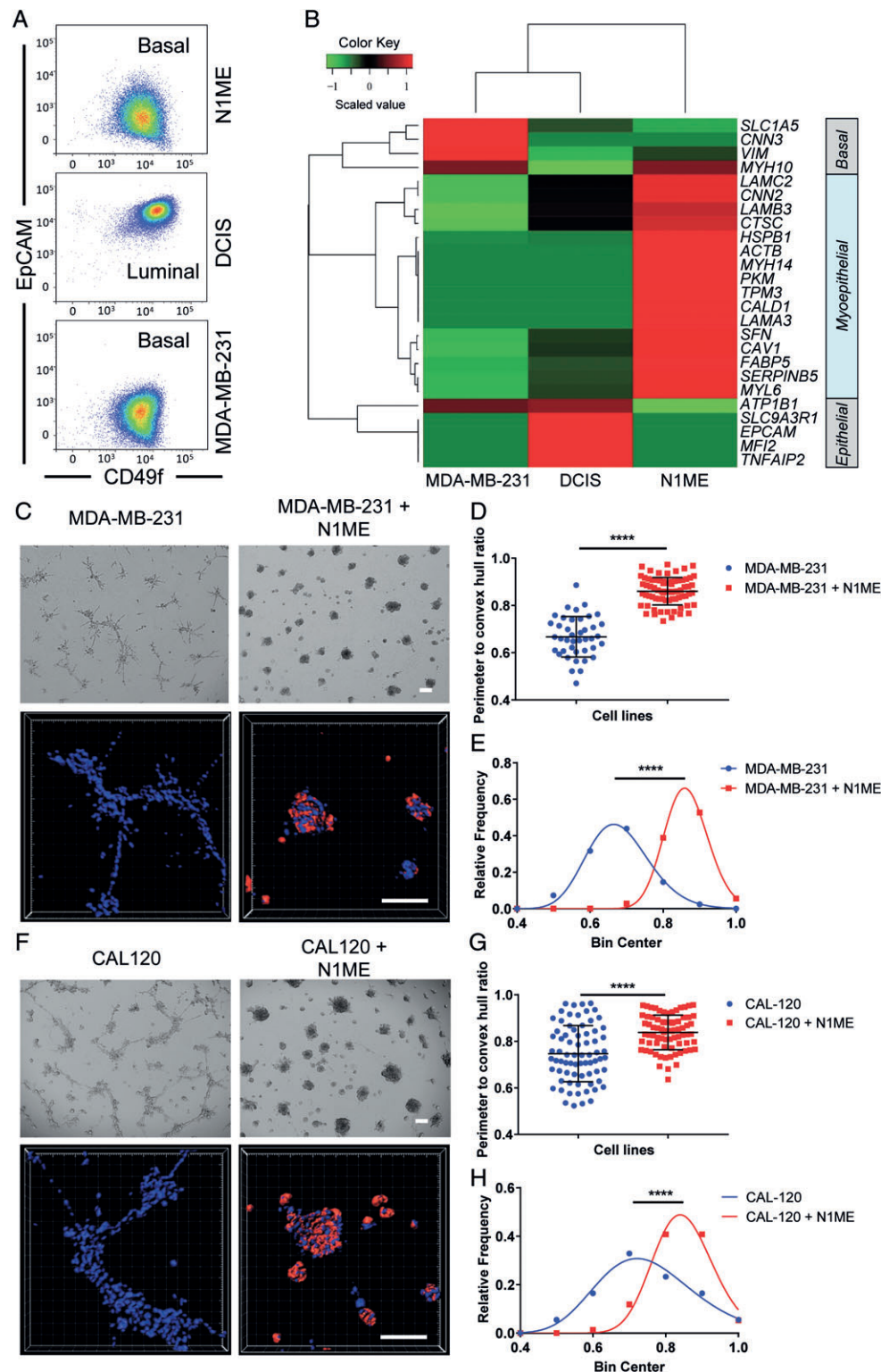


Figure 2. Characterization and 3D modelling of breast myoepithelial and cancer cell lines. (A) Cell surface EpCAM and CD49f expression determined on cell lines using flow cytometry analysis. Plots show EpCAM and CD49f expression on cells after gating on viable cells that are Lin-negative (CD45[−] CD235a[−] CD31[−]); N1ME: CD49^{fl}/EpCAM^{low}; DCIS.com: CD49^{fl}/EpCAM^{hi}; MDA-MB-231: CD49^{fl}/EpCAM^{low}. (B) Heat map depicting the correlation expression profile of select differentially expressed proteins in myoepithelial cellular proteomics (N1ME) in comparison to luminal (DCIS.com) and basal (MDA-MB-231) cellular models. Data represent differential abundance based on normalized LFQ intensity values ($n = 3$). Bright field and confocal images, rendered in Imaris, of (C) MDA-MB-231 and (F) CAL120 invasive breast cancer cells (blue, Hoechst-stained) grown on reconstituted basement membrane with overlay alone, and co-cultured with N1ME cherry-labelled myoepithelial cells (red) for 7 days. Representative images of $n = 3$. Scale bars represent 200 μ m. (D, G) Differences in the invasive growth of 3D cultures were determined by calculating the ratio between the perimeter and convex hull of each colony (circularity). A value of 1 indicates a smooth object; as the value moves away from 1 towards 0, the number and/or size of protrusions from the colony is increased. (E, H) Frequency distribution of population data under log Gaussian fit. A bin center closer to 1 indicated a smooth colony surface. Comparison of the center of each curve was statistically analyzed. **** $p < 0.0001$. $n = 3$.

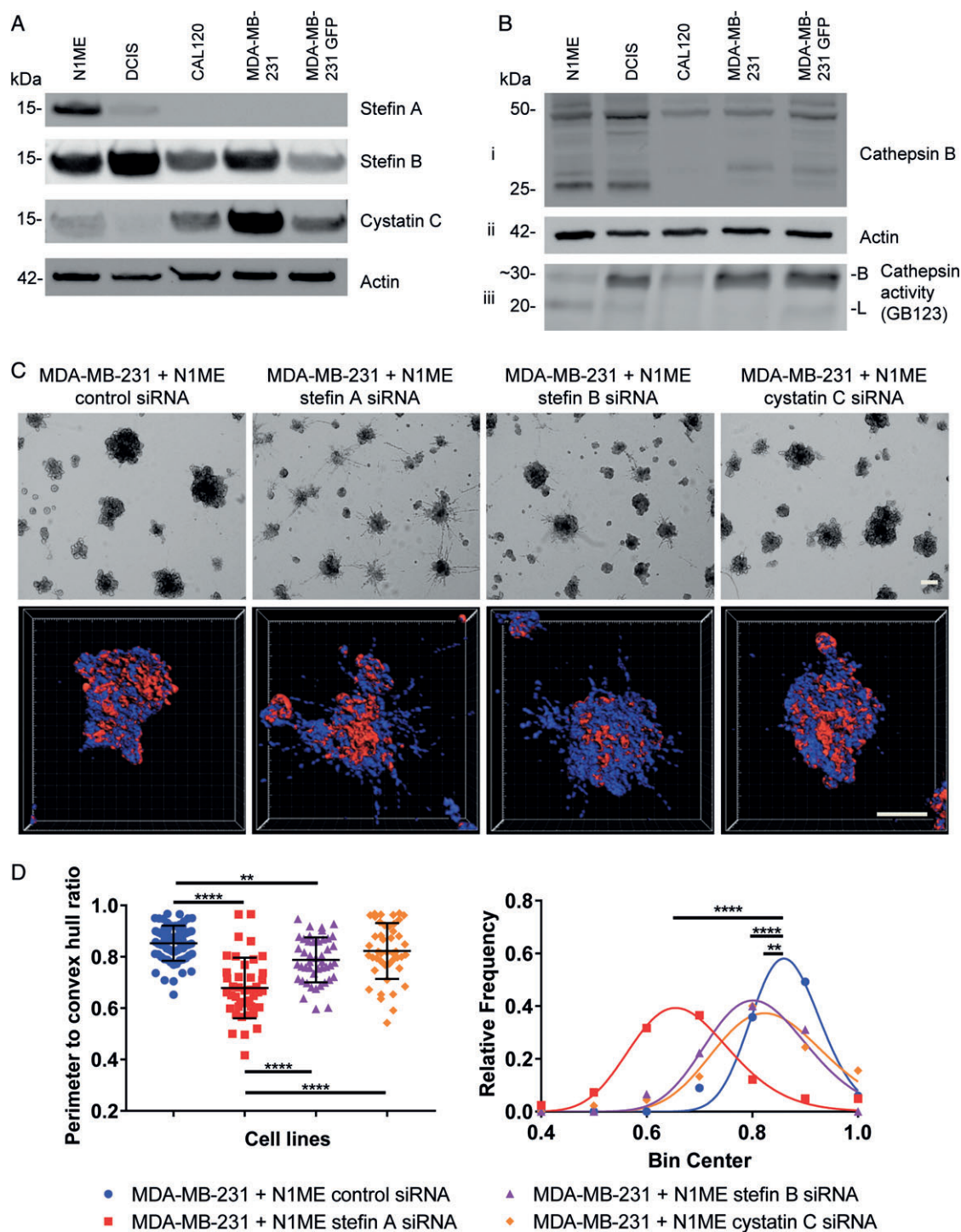


Figure 3. siRNA knockdown of cathepsin inhibitors affects myoepithelial cells' ability to control invasive breast cancer cells. (A) Expression of steffin A, steffin B, and cystatin C detected by western blotting in whole cell lysates of human breast myoepithelial and epithelial cell lines. β -Actin was used as a loading control. (Bi) Expression of cathepsin B detected by western blotting. The 28 and 30 kDa bands reflect the heavy chain of double-chain and single-chain forms of mature cathepsin B. (Bii) β -Actin was used as a loading control. (Biii) Cathepsin B and L activity was determined by the use of an activity-based probe (GB123). Blots are representative of three independent experiments. (C) 3D co-culture of MDA-MB-231 cells with N1ME cherry-labeled myoepithelial cells, with siRNA knockdown of cathepsin inhibitors steffin A, steffin B, and cystatin C or siRNA control. Scale bars represent 200 μ m. (D) Quantification of invasive outgrowths as described in Figure 2. ** $p < 0.01$; **** $p < 0.0001$. $n = 2$.

Given the high levels of cystatins in the myoepithelial cell line, a small siRNA screen was conducted to test their function in N1ME cells in 3D (supplementary material, Figure S2K–M). Although the siRNA control N1ME lines blocked MDA-MB-231 cell invasion,

knockdown of steffin A could not restrain tumor invasion (Figure 3C, D). The impact of steffin A was greater than that observed with knockdown of steffin B and cystatin C, where only very minor tumor outgrowths or no invasion was observed, respectively (Figure 3C, D).

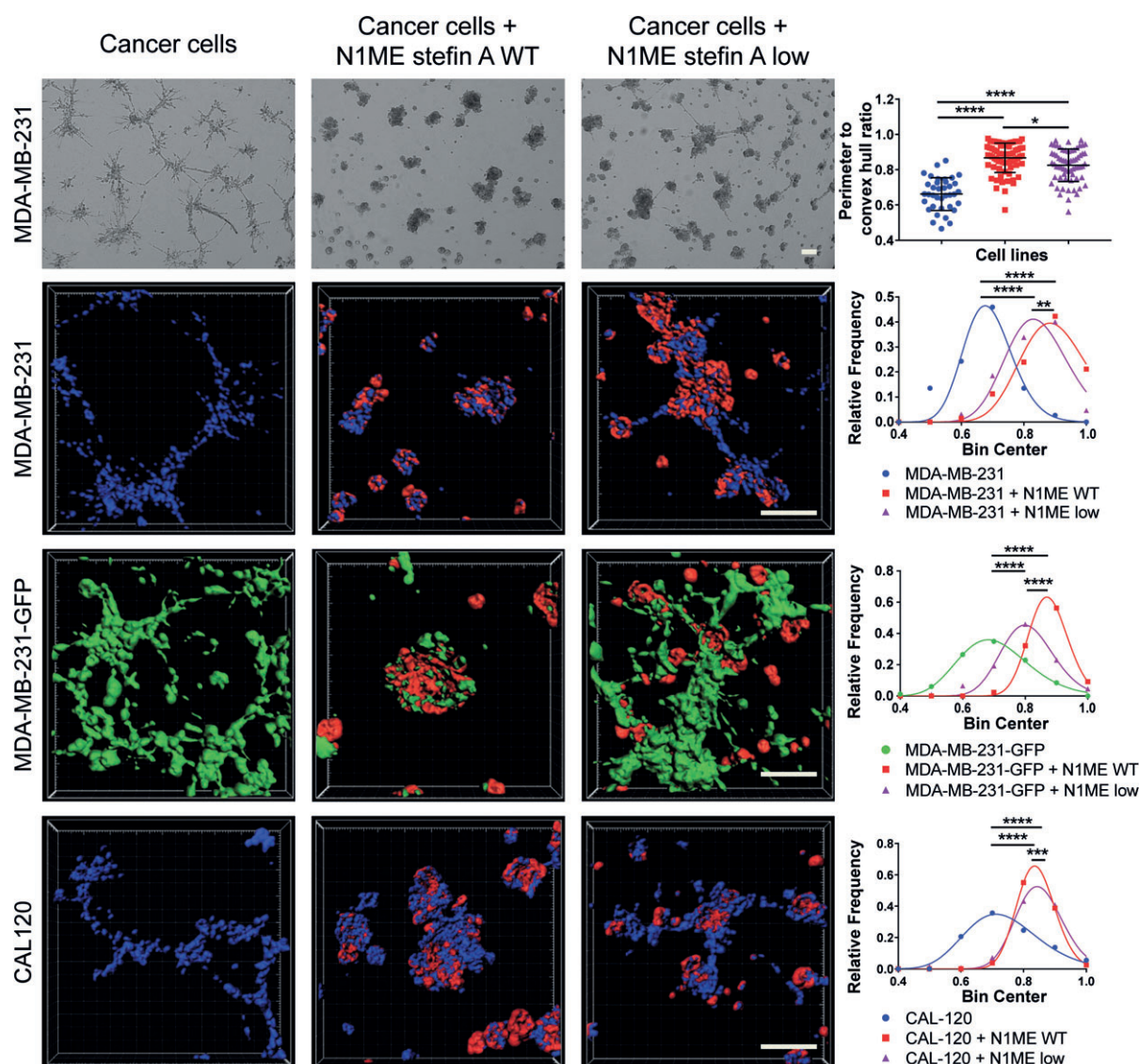


Figure 4. Decreased myoepithelial stefin A expression promotes MDA-MB-231 invasion in 3D co-culture. Breast cancer cells cultured alone, co-cultured with N1ME stefin A wild-type, or co-cultured with N1ME stefin A-low cells. Top panel: bright field images of MDA-MB-231 (not labeled) and co-cultured with myoepithelial cells. Bottom panels: confocal images, rendered in Imaris, of MDA-MB-231 (blue, Hoechst-stained), MDA-MB-231-GFP (green), or CAL120 (blue, Hoechst-stained) alone or co-cultured with myoepithelial cells (red). Scale bars represent 200 μm . Right panels: quantification of invasive outgrowths as described in Figure 2. * $p < 0.05$; ** $p < 0.01$; *** $p < 0.001$; **** $p < 0.0001$. $n = 3$. Bright field images of other cultures and further quantification are provided in the supplementary material, Figures S3F–H.

Given that stefin A expression was high in the N1ME cells and correlated inversely with cathepsin B activity (Figure 3A, B), and that knockdown had the greatest impact on tumor cell invasion, we wanted to further confirm its invasion-suppressive function by using stable gene editing of the N1ME cell lines.

Stefin A-low (heterozygote null) N1ME cell lines were created using transcription activator-like effector nucleases (TALENs), resulting in a 60–80% decrease in stefin A expression and an increase in cathepsin B activity (supplementary material, Figure S3A–C). Although a reduction in stefin A expression did not impact myoepithelial cell proliferation or morphology (supplementary material, Figure S3D, E), it had a dramatic effect in 3D co-culture. The stefin A-low N1ME cells failed to inhibit MDA-MB-231 cell invasion to

the extent observed with wild-type (WT) N1ME cells (Figure 4), confirming the results achieved with the siRNA experiments. This was confirmed using both unlabeled and GFP-labeled MDA-MB-231 cells and the CAL120 cell line (Figure 4 and supplementary material, Figure S3F–H). Together, these findings demonstrate the importance of stefin A in the myoepithelial-driven suppression of tumor cell invasion.

To confirm that the alteration in phenotype was due to the role of stefin A as a cathepsin inhibitor, we treated MDA-MB-231 cells alone or co-cultured with the stefin A-low N1ME line with cathepsin B-specific (CA-074) and pan-cysteine cathepsin (JPM-OEt) inhibitors. We reasoned that given stefin A is secreted from N1ME cells (supplementary material, Figure S4A), addition of inhibitors to the media was feasible. Indeed, we

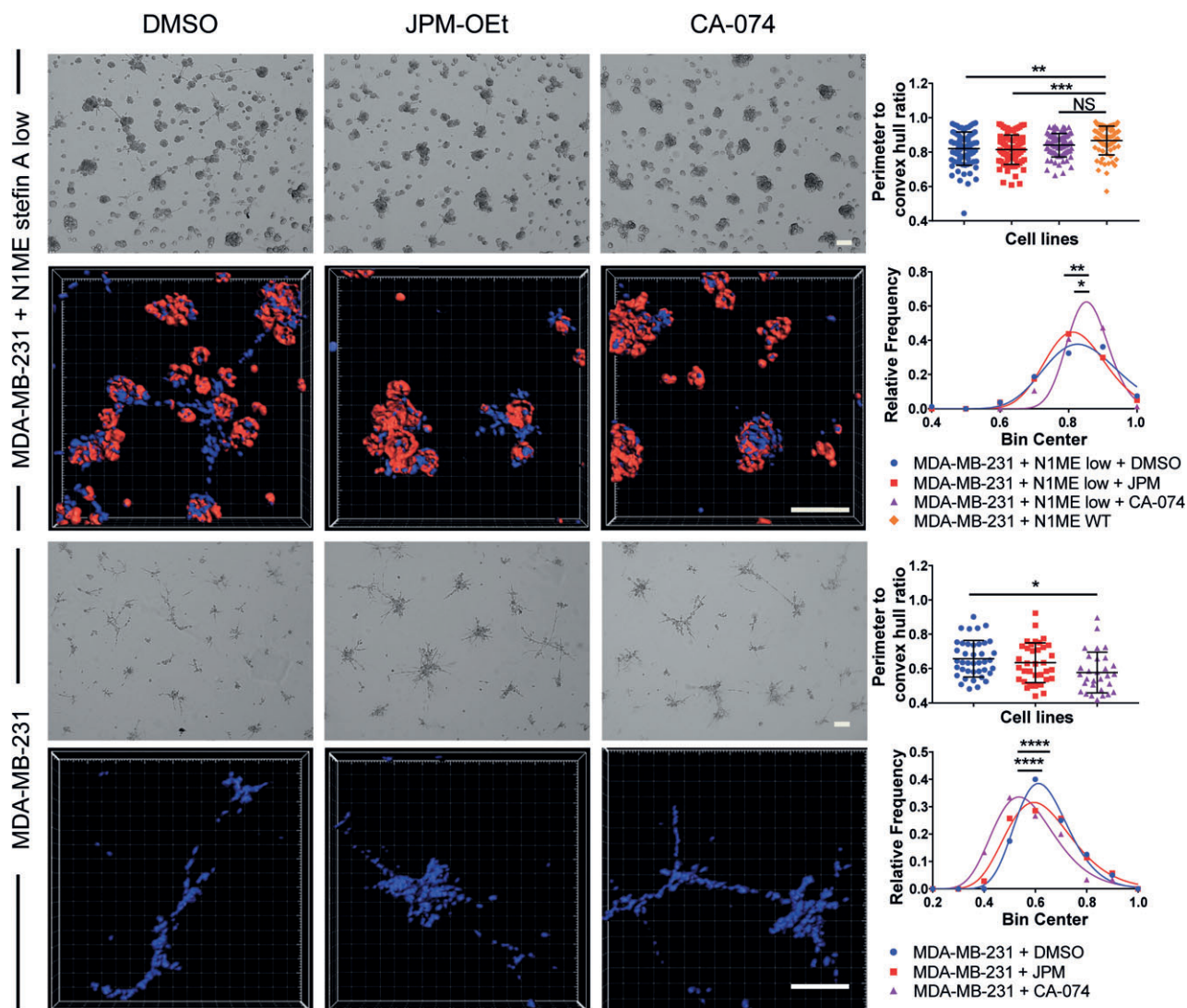


Figure 5. Cysteine cathepsin inhibitors revert the invasive state of MDA-MB-231 cells in 3D co-culture with stefin A-low myoepithelial cells. MDA-MB-231 cells alone or in 3D co-culture with N1ME stefin A-low cells were treated with cysteine cathepsin inhibitors CA-074, JPM-OEt, or DMSO control. Inhibitors were replenished every 48 h. Bright field images and confocal images, rendered in Imaris, of MDA-MB-231 cells (blue, Hoechst-stained) alone or co-cultured with stefin A-low myoepithelial cells (red). Scale bars represent 200 μ m. Right panels: quantification of invasive outgrowths as described in Figure 2. NS = not significant. * $p < 0.05$; ** $p < 0.01$; *** $p < 0.001$; **** $p < 0.0001$. $n = 3$.

observed that CA-074 treatment rescued the phenotype caused by stefin A loss, reverting the invasive protrusions of the co-cultures back to the DCIS-like state observed using WT N1ME cells (Figure 5, top panels). JPM-OEt also reverted the invasive protrusions in the co-cultures; however, this was not significant compared with vehicle control treatment (Figure 5). Importantly, this phenotype was not observed in the absence of myoepithelial cells. Use of inhibitors did not inhibit invasion of the MDA-MB-231 cells cultured in the absence of N1ME cells; in fact, it made the breast cancer cells more invasive (Figure 5, bottom panels). This was also observed using N1ME conditioned media or recombinant stefin A (supplementary material, Figure S4B, C), where tumor cell invasion was not suppressed. These results indicate that both the physical presence of myoepithelial cells and intact stefin A expression are required to block invasion, suggesting

that stefin A loss alters the tumor-suppressive function of the myoepithelial cells.

Stefin A expression in DCIS

Our studies utilizing the N1ME cell line suggest that stefin A is highly abundant in normal myoepithelial cells. To confirm our findings clinically, stefin A expression was assessed in breast tissue derived from cancer-free women. Indeed, we detected abundant stefin A expressed in the myoepithelial cells surrounding normal ducts (Figure 6A, B). Expression patterns were confirmed by two independent stefin A antibodies (supplementary material, Figure S5A). We then interrogated cell-specific stefin A expression in early-stage tumorigenesis using a tissue microarray comprising sections of more than 800 lesions encompassing benign ducts, usual ductal hyperplasia, and low, intermediate or high nuclear grade DCIS. The myoepithelial expression

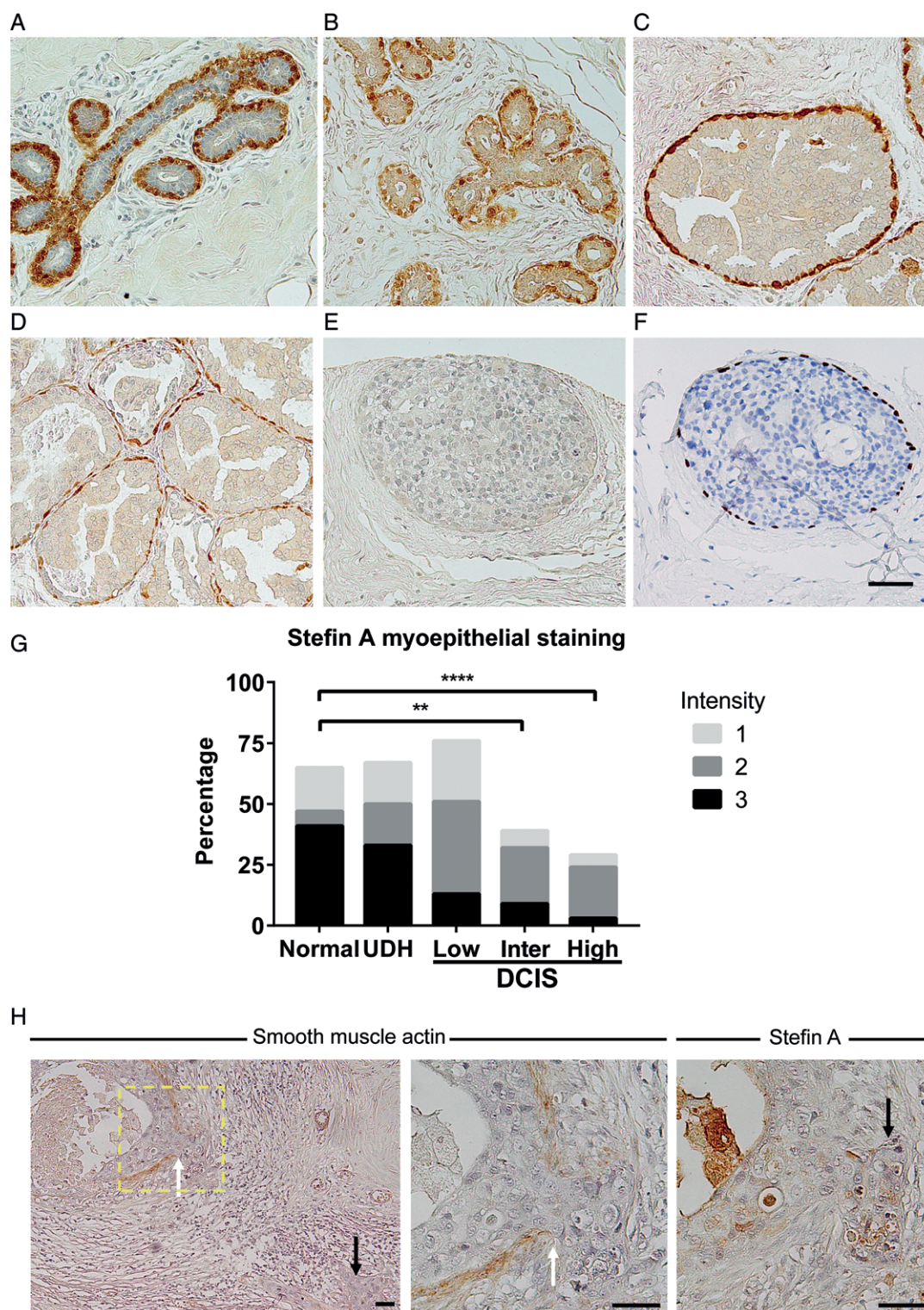


Figure 6. Stefín A expression in human normal and carcinoma tissue. Sections of formalin-fixed, paraffin-embedded tissue were stained with rabbit anti-human stefín A and visualized with DAB (brown). All sections were counterstained with hematoxylin (blue nuclei). Expression of stefín A in myoepithelial cells surrounding (A, B) normal breast ducts and (C) DCIS lesions. (D) Aberrant or (E) no myoepithelial stefín A expression in DCIS lesions. (F) Mouse anti-human p63 was used as a positive control for the presence of myoepithelial cells in all tissues. (G) Myoepithelial stefín A expression was pathologist-scored and compared between groups: normal, usual ductal hyperplasia (UDH), and DCIS grades low, intermediate (inter), and high. The percentage of patients with the scoring intensity is shown. Comparison by chi-square test on patient numbers in each group. **** $p < 0.0001$; ** $p < 0.01$. $n = 138$ patients. (H) DCIS tissue with identified micro-invasive regions were stained with rabbit anti-human stefín A or smooth muscle actin (SMA) and visualized with DAB (brown staining). The presence of myoepithelial cells was confirmed by SMA positivity on serial sections. White arrows indicate the focal break in the myoepithelial boundary. Black arrows indicate invasive cells. Scale bars represent 50 μm .

of stefin A was retained in hyperplastic and low-grade DCIS lesions (Figure 6C, D), yet was reduced or absent in many intermediate- and high-grade DCIS lesions (Figure 6E). The distinction between DCIS and invasion is the presence of the myoepithelial cell layer [4], and myoepithelial marker immunohistochemistry (IHC) is used widely in diagnostic clinical practice to aid in this distinction. To rule out loss or attenuation of the myoepithelial layer in stefin A-negative lesions, serial sections were stained with p63 (Figure 6F), a nuclear myoepithelial marker. Only p63-positive samples were included in the analysis. Importantly, stefin A expression correlated inversely with DCIS grade (Figure 6G), yet did not correlate with ER, PR, histological grade or tumor size (supplementary material, Table S3A). A fraction (35%) of normal ducts lacked myoepithelial stefin A, and currently, the implications of this loss on future breast cancer risk are unknown.

The negative correlation between stefin A expression and DCIS grade was restricted to myoepithelial cells. Evaluation of stefin A expression in the neoplastic epithelium (supplementary material, Figure S5B) revealed an increase in DCIS lesions in general, and an increase with grade (supplementary material, Figure S5C and Table S3B). This suggests that the role of stefin A in early tumorigenesis is likely cell-dependent and therefore it is the loss of myoepithelial cell stefin A surrounding DCIS lesions that is most implicated in the DCIS-to-invasive carcinoma transition. In support of this, cathepsin inhibition caused MDA-MB-231 cancer cells to become more invasive in 3D culture (Figure 5), and knockout of stefin A in the DCIS.com cell line did not affect cell growth or invasion in 3D culture (supplementary material, Figure S5D–F).

Patients diagnosed with high-grade DCIS have an increased risk of local invasion compared with low-grade lesions [34]. However, as clinical follow-up on the subsequent development of invasive carcinoma (fortunately, a rare event as patients received modern treatment) was not available, we investigated stefin A expression in high-grade DCIS lesions with associated micro-invasive regions, the earliest phase of invasion. Micro-invasion is defined as an invasive focus measuring no more than 1 mm. In this study, alpha-smooth muscle actin (SMA), a cytoplasmic/cytoskeletal myoepithelial marker, was used to highlight the presence of the myoepithelial cells, including identification of any small focal breaks in the myoepithelial cell boundary (Figure 6H, white arrows). In line with an association between stefin A loss and tumor invasion, it was observed that DCIS lesions with micro-invasion did not express myoepithelial stefin A (Figure 6H and supplementary material, Figure S6). This suggests that the decrease in myoepithelial stefin A expression predicts invasion and that loss of stefin A may precede myoepithelial cell loss in invasive lesions. This supports our findings with the 3D co-culture models that intact stefin A expression is important in myoepithelial-specific suppression of tumor invasion.

Discussion

This study implicates myoepithelial stefin A in preventing the progression of DCIS to invasion. We reveal that targeted loss of stefin A in myoepithelial cells is sufficient to promote or restore tumor cell invasion in a 3D DCIS-like model developed in the laboratory. This function relies on the cathepsin inhibitory role of stefin A, as cathepsin inhibitors could rescue this phenotype, and therefore future studies will aim to explore the role of cathepsin B and its substrates in the early steps of the progression from DCIS to invasion. Critically, here we report for the first time that stefin A is highly expressed in myoepithelial cells of low-grade DCIS lesions, those that have the lowest risk of local recurrence within 10 years [34]. These data suggest that myoepithelial stefin A has an important suppressive function in the DCIS-to-invasive carcinoma transition and that it is worthy of further investigation as a prognostic marker, to distinguish patients who are at a decreased risk of developing invasive breast cancer and could therefore be spared from adjuvant therapies.

Previous studies on the involvement of stefin A in tumorigenesis are contradictory, with reports that it is a tumor suppressor in some cancers [22,35,36] yet a malignant marker in others [37–39]. However, investigations into the cell-specific expression and function of stefin A in early tumorigenesis are limited. Here, we report that a critical source of stefin A at the DCIS stage is from myoepithelial cells. A study by Lee *et al.* reported that stefin A expression decreases in tumor cells of invasive lesions compared with DCIS and that stefin A reduction promotes tumor invasion [40]. The comparison of DCIS samples to invasive lesions did not allow an assessment of whether stefin A loss can occur in DCIS lesions before invasion, nor did it assess changes to the myoepithelial compartment as we have investigated in the current study. In our studies, although other cathepsin inhibitors (stefin B and cystatin C) were not exclusively expressed in myoepithelial cells, knockdown of stefin B in myoepithelial cells did promote tumor cell invasion. There have been some reports suggestive of a role of these inhibitors in breast cancer progression. Cystatin C expression has been documented to correlate with larger breast tumor size [41], while a study has shown that low stefin B levels correlate with shorter disease-free survival in breast cancer patients [42]. However, in a mouse model of breast cancer, stefin B loss decreased tumor burden [43], conflicting with the patient prognostic data. Together, these studies warrant future cell-specific investigations into the role of cathepsin inhibitors during breast cancer initiation and progression.

Despite considerable efforts to identify tumor cell markers that predict DCIS progression and allow individualized therapies, there are limited biomarkers to date that warrant further evaluation. This is in part due to studies that reveal minimal genetic and transcriptional differences between tumor cells in DCIS and invasive

lesions [44,45]. A commercial test currently available for predicting disease recurrence in women with early-stage breast cancer is the Oncotype DX® Recurrence Score (RS), based on the expression of 21 genes [46]. This has now been adapted for DCIS, whereby an Oncotype DX DCIS® score has been developed [47]. While this test can aid in patient treatment decisions for those with low or high scores, 16–25% of patients will fall into the ‘intermediate’ score range, indicating that it is ‘unclear’ whether they will receive benefits from adjuvant therapy [46,47]. Ongoing trials are therefore required to determine the utility of these scores in discriminating indolent and high-risk DCIS lesions. Given the genetic similarities between tumor cells of DCIS and those of invasive lesions, prognostic markers in the surrounding microenvironment may hold great promise.

Our finding that stefin A is decreased in high-grade and micro-invasive lesions, yet abundant in low-grade DCIS lesions, suggests its potential as a prognostic marker for discriminating DCIS lesions with a decreased risk of local recurrence. This may be particularly important in patients with low- and intermediate-grade DCIS who have a very small risk of relapse and may not even need surgical intervention. Culmination of stefin A into an affordable next-generation or IHC-based assay may be beneficial and cost-effective, and will need to be tested in larger follow-up cohorts.

Acknowledgements

We gratefully thank Peter Lock of the LIMS Microscopy and Imaging Facility, the staff at La Trobe University Central Animal House for technical assistance, and the La Trobe Comprehensive Proteomics Platform for access to equipment and expertise employed in this study. We express our gratitude to Dr Elgene Lim for the gift of the CAL120 cell line. We also thank Dr Kaylene Simpson and Dr Iva Nikolic from the Peter MacCallum Cancer Centre for their assistance with siRNA. This work was supported by grant funding from the National Health and Medical Research Council (NHMRC) (BSP 1047748 and 1127754); fellowship support to BSP from the ARC (FT130100671), DAS from the NHMRC (1070916), and SOT from the NBCF (Practitioner Fellowship PRAC-16-006); and scholarship support from the Cancer Council Victoria (to HMD). Support from the Sydney Breast Cancer Foundation is also gratefully acknowledged.

Author contributions statement

The authors contributed in the following way: conceptualization, HMD, LEEM, and BSP; methodology, HMD, JR, LEEM, DS, and BSP; software, CJN; formal analysis, HMD, TJM, DWG, and CJN; investigation, HMD, JR, AS, ER, NKB, KLB, MC, and DWG; data input, CIS; resources, KP, MH, MB, AM, CSL,

AH, SAOT, BFS, and BSP; writing – original draft, HMD and BSP; writing – review and editing, HMD, BSP, SAOT, LEEM, JR, DAS, DWG, KLB, TJM, and CSL; funding acquisition, BSP; and supervision, BSP and LEEM.

References

- Downs-Holmes C, Silverman P. Breast cancer: overview & updates. *Nurse Pract* 2011; **36**: 20–26.
- Van Cleef A, Altintas S, Huizing M, *et al.* Current view on ductal carcinoma *in situ* and importance of the margin thresholds: a review. *Facts Views Vis Obgyn* 2014; **6**: 210–218.
- Collins LC, Achacoso N, Haque R, *et al.* Risk factors for non-invasive and invasive local recurrence in patients with ductal carcinoma *in situ*. *Breast Cancer Res Treat* 2013; **139**: 453–460.
- Polyak K, Hu M. Do myoepithelial cells hold the key for breast tumor progression? *J Mammary Gland Biol Neoplasia* 2005; **10**: 231–247.
- Deane HW, Forbes A. Myoepithelial cells and their function. *J Appl Physiol* 1956; **9**: 495–496.
- Gudjonsson T, Adriance M, Sternlicht M, *et al.* Myoepithelial cells: their origin and function in breast morphogenesis and neoplasia. *J Mammary Gland Biol Neoplasia* 2005; **10**: 261–272.
- Gudjonsson T, Ronnov-Jessen L, Villadsen R, *et al.* Normal and tumor-derived myoepithelial cells differ in their ability to interact with luminal breast epithelial cells for polarity and basement membrane deposition. *J Cell Sci* 2002; **115**: 39–50.
- Sternlicht MD, Kedeshian P, Shao ZM, *et al.* The human myoepithelial cell is a natural tumor suppressor. *Clin Cancer Res* 1997; **3**: 1949–1958.
- Sternlicht MD, Barsky SH. The myoepithelial defense: a host defense against cancer. *Med Hypotheses* 1997; **48**: 37–46.
- Barsky SH, Karlin NJ. Myoepithelial cells: autocrine and paracrine suppressors of breast cancer progression. *J Mammary Gland Biol Neoplasia* 2005; **10**: 249–260.
- Turk V, Stoka V, Vasiljeva O, *et al.* Cysteine cathepsins: from structure, function and regulation to new frontiers. *Biochim Biophys Acta* 2012; **1824**: 68–88.
- Mohamed MM, Sloane BF. Cysteine cathepsins: multifunctional enzymes in cancer. *Nat Rev Cancer* 2006; **6**: 764–775.
- Gocheva V, Zeng W, Ke D, *et al.* Distinct roles for cysteine cathepsin genes in multistage tumorigenesis. *Genes Dev* 2006; **20**: 543–556.
- Vasiljeva O, Papazoglou A, Kruger A, *et al.* Tumor cell-derived and macrophage-derived cathepsin B promotes progression and lung metastasis of mammary cancer. *Cancer Res* 2006; **66**: 5242–5250.
- Kleer CG, Bloushtain-Qimron N, Chen Y-H, *et al.* Epithelial and stromal cathepsin K and CXCL14 expression in breast tumor progression. *Clin Cancer Res* 2008; **14**: 5357–5367.
- Buck MR, Karustis DG, Day NA, *et al.* Degradation of extracellular-matrix proteins by human cathepsin B from normal and tumour tissues. *Biochem J* 1992; **282**: 273–278.
- Joyce JA, Baruch A, Chehade K, *et al.* Cathepsin cysteine proteases are effectors of invasive growth and angiogenesis during multistage tumorigenesis. *Cancer Cell* 2004; **5**: 443–453.
- Kern U, Wischniewski V, Biniossek ML, *et al.* Lysosomal protein turnover contributes to the acquisition of TGFβ₁ induced invasive properties of mammary cancer cells. *Mol Cancer* 2015; **14**: 39.
- Sevenich L, Werner F, Gajda M, *et al.* Transgenic expression of human cathepsin B promotes progression and metastasis of polyoma-mid-T-induced breast cancer in mice. *Oncogene* 2011; **30**: 54–64.
- Withana NP, Blum G, Sameni M, *et al.* Cathepsin B inhibition limits bone metastasis in breast cancer. *Cancer Res* 2012; **72**: 1199–1209.

21. Barrett AJ. The cystatins: a new class of peptidase inhibitors. *Trends Biochem Sci* 1987; **12**: 193–196.
22. Parker BS, Ciocca DR, Bidwell BN, et al. Primary tumour expression of the cysteine cathepsin inhibitor stefin A inhibits distant metastasis in breast cancer. *J Pathol* 2008; **214**: 337–346.
23. Allinen M, Beroukhi R, Cai L, et al. Molecular characterization of the tumor microenvironment in breast cancer. *Cancer Cell* 2004; **6**: 17–32.
24. Miller FR, Santner SJ, Tait L, et al. MCF10DCIS.com xenograft model of human comedo ductal carcinoma *in situ*. *J Natl Cancer Inst* 2000; **92**: 1185–1186.
25. Lim E, Vaillant F, Wu D, et al. Aberrant luminal progenitors as the candidate target population for basal tumor development in *BRCA1* mutation carriers. *Nat Med* 2009; **15**: 907–913.
26. Schindelin J, Arganda-Carreras I, Frise E, et al. Fiji: an open-source platform for biological-image analysis. *Nat Methods* 2012; **9**: 676–682.
27. Edgington-Mitchell LE, Rautela J, Duivenvoorden HM, et al. Cysteine cathepsin activity suppresses osteoclastogenesis of myeloid-derived suppressor cells in breast cancer. *Oncotarget* 2015; **6**: 27008–27022.
28. Blum G, von Degenfeld G, Merchant MJ, et al. Noninvasive optical imaging of cysteine protease activity using fluorescently quenched activity-based probes. *Nat Chem Biol* 2007; **3**: 668–677.
29. Verdoes M, Oresic Bender K, Segal E, et al. Improved quenched fluorescent probe for imaging of cysteine cathepsin activity. *J Am Chem Soc* 2013; **135**: 14726–14730.
30. Zardawi SJ, Zardawi I, McNeil CM, et al. High Notch1 protein expression is an early event in breast cancer development and is associated with the HER-2 molecular subtype. *Histopathology* 2010; **56**: 286–296.
31. Lin EY, Jones JG, Li P, et al. Progression to malignancy in the polyoma middle T oncoprotein mouse breast cancer model provides a reliable model for human diseases. *Am J Pathol* 2003; **163**: 2113–2126.
32. Sameni M, Cavallo-Medved D, Franco OE, et al. Pathomimetic avatars reveal divergent roles of microenvironment in invasive transition of ductal carcinoma *in situ*. *Breast Cancer Res* 2017; **19**: 56.
33. Jones C, Mackay A, Grigoriadis A, et al. Expression profiling of purified normal human luminal and myoepithelial breast cells: identification of novel prognostic markers for breast cancer. *Cancer Res* 2004; **64**: 3037–3045.
34. Wood WC, Alvarado M, Buchholz DJ, et al. The current clinical value of the DCIS score. *Oncology (Williston Park)* 2014; **28**(suppl 2): C2, 1–8, C3.
35. Stojan P, Oblak I, Svetic B, et al. Cysteine proteinase inhibitor cystatin C in squamous cell carcinoma of the head and neck: relation to prognosis. *Br J Cancer* 2004; **90**: 1961–1968.
36. Stojnik T, Zaje I, Bervar A, et al. Cathepsin B and its inhibitor stefin A in brain tumors. *Pflugers Arch* 2000; **439**: R122–R123.
37. Chang KP, Wu CC, Chen HC, et al. Identification of candidate nasopharyngeal carcinoma serum biomarkers by cancer cell secretome and tissue transcriptome analysis: potential usage of cystatin A for predicting nodal stage and poor prognosis. *Proteomics* 2010; **10**: 2644–2660.
38. Tang M, Ou N, Li C, et al. Expression and prognostic significance of macrophage inflammatory protein-3 alpha and cystatin A in nasopharyngeal carcinoma. *Biomed Res Int* 2015; **2015**: 617143.
39. Kuopio T, Kankaanranta A, Jalava P, et al. Cysteine proteinase inhibitor cystatin A in breast cancer. *Cancer Res* 1998; **58**: 432–436.
40. Lee S, Stewart S, Nagtegaal I, et al. Differentially expressed genes regulating the progression of ductal carcinoma *in situ* to invasive breast cancer. *Cancer Res* 2012; **72**: 4574–4586.
41. Vigneswaran N, Wu J, Muller S, et al. Expression analysis of cystatin C and M in laser-capture microdissected human breast cancer cells – a preliminary study. *Pathol Res Pract* 2005; **200**: 753–762.
42. Levicar N, Kos J, Blejec A, et al. Comparison of potential biological markers cathepsin B, cathepsin L, stefin A and stefin B with urokinase and plasminogen activator inhibitor-1 and clinicopathological data of breast carcinoma patients. *Cancer Detect Prev* 2002; **26**: 42–49.
43. Butinar M, Prebanda MT, Rajkovic J, et al. Stefina B deficiency reduces tumor growth via sensitization of tumor cells to oxidative stress in a breast cancer model. *Oncogene* 2013; **33**: 3392–3400.
44. Moelans CB, de Wegers RA, Monsuurs HN, et al. Molecular differences between ductal carcinoma *in situ* and adjacent invasive breast carcinoma: a multiplex ligation-dependent probe amplification study. *Cell Oncol (Dordr)* 2011; **34**: 475–482.
45. Porter D, Lahti-Domenici J, Keshaviah A, et al. Molecular markers in ductal carcinoma *in situ* of the breast. *Mol Cancer Res* 2003; **1**: 362–375.
46. Martei YM, Matro JM. Identifying patients at high risk of breast cancer recurrence: strategies to improve patient outcomes. *Breast Cancer (Dove Med Press)* 2015; **7**: 337–343.
47. Rakovitch E, Nofech-Mozes S, Hanna W, et al. A population-based validation study of the DCIS score predicting recurrence risk in individuals treated by breast-conserving surgery alone. *Breast Cancer Res Treat* 2015; **152**: 389–398.
- *48. Greening DW, Ji H, Chen M, et al. Secreted primary human malignant mesothelioma exosome signature reflects oncogenic cargo. *Sci Rep* 2016; **6**: 32643.
- *49. Tauro BJ, Greening DW, Mathias RA, et al. Comparison of ultracentrifugation, density gradient separation, and immunoaffinity capture methods for isolating human colon cancer cell line LIM1863-derived exosomes. *Methods* 2012; **56**: 293–304.
- *50. Tauro BJ, Greening DW, Mathias RA, et al. Two distinct populations of exosomes are released from LIM1863 colon carcinoma cell-derived organoids. *Mol Cell Proteomics* 2013; **12**: 587–598.
- *51. Gopal SK, Greening DW, Mathias RA, et al. YBX1/YB-1 induces partial EMT and tumorigenicity through secretion of angiogenic factors into the extracellular microenvironment. *Oncotarget* 2015; **6**: 13718–13730.
- *52. Greening DW, Nguyen HP, Elgass K, et al. Human endometrial exosomes contain hormone-specific cargo modulating trophoblast adhesive capacity: insights into endometrial–embryo interactions. *Biol Reprod* 2016; **94**: 38.
- *53. Gorshkov V, Verano-Braga T, Kjeldsen F. SuperQuant: a data processing approach to increase quantitative proteome coverage. *Anal Chem* 2015; **87**: 6319–6327.
- *54. Cox J, Mann M. MaxQuant enables high peptide identification rates, individualized p.p.b.-range mass accuracies and proteome-wide protein quantification. *Nat Biotechnol* 2008; **26**: 1367–1372.
- *55. Greening DW, Kapp EA, Ji H, et al. Colon tumour secretome: insights into endogenous proteolytic cleavage events in the colon tumour microenvironment. *Biochim Biophys Acta* 2013; **1834**: 2396–2407.
- *56. Brosch M, Yu L, Hubbard T, et al. Accurate and sensitive peptide identification with Mascot Percolator. *J Proteome Res* 2009; **8**: 3176–3181.
- *57. Nesvizhskii AI, Aebersold R. Interpretation of shotgun proteomic data: the protein inference problem. *Mol Cell Proteomics* 2005; **4**: 1419–1440.
- *58. Keller A, Nesvizhskii AI, Kolker E, et al. Empirical statistical model to estimate the accuracy of peptide identifications made by MS/MS and database search. *Anal Chem* 2002; **74**: 5383–5392.
- *59. Lubner CA, Cox J, Lauterbach H, et al. Quantitative proteomics reveals subset-specific viral recognition in dendritic cells. *Immunity* 2010; **32**: 279–289.
- *60. Benjamini Y, Hochberg Y. Controlling the false discovery rate: a practical and powerful approach to multiple testing. *J R Stat Soc Ser B Stat Methodol* 1995; **57**: 289–300.

- *61. Tauro BJ, Mathias RA, Greening DW, *et al.* Oncogenic H-ras reprograms Madin–Darby canine kidney (MDCK) cell-derived exosomal proteins following epithelial–mesenchymal transition. *Mol Cell Proteomics* 2013; **12**: 2148–2159.
- *62. Huang da W, Sherman BT, Lempicki RA. Systematic and integrative analysis of large gene lists using DAVID bioinformatics resources. *Nat Protoc* 2009; **4**: 44–57.
- *63. Sander JD, Maeder ML, Reyon D, *et al.* ZiFiT (zinc finger targeter): an updated zinc finger engineering tool. *Nucleic Acids Res* 2010; **38**: W462–W468.
- *64. Reyon D, Tsai SQ, Khayter C, *et al.* FLASH assembly of TAL-ENs for high-throughput genome editing. *Nat Biotechnol* 2012; **30**: 460–465.
- *65. Reljic B, Stroud DA. Screening strategies for TALEN-mediated gene disruption. *Methods Mol Biol* 2016; **1419**: 231–252.
- *66. Vichai V, Kirtikara K. Sulforhodamine B colorimetric assay for cytotoxicity screening. *Nat Protoc* 2006; **1**: 1112–1116.
- *Cited only in supplementary material.

SUPPLEMENTARY MATERIAL ONLINE

Supplementary materials and methods

Supplementary figure legends

Figure S1. Progression of PyMT mouse model and tumour cell proliferation status between DMSO- and CA-074-treated mice

Figure S2. N1ME characterization, control 2D and 3D co-culture experiments, and quantification

Figure S3. Generation of myoepithelial stefin A-low cell lines

Figure S4. 3D co-culture control experiments and stefin A inhibition of cathepsin B

Figure S5. Expression of stefin A in DCIS tissue

Figure S6. Expression of stefin A in micro-invasive tissues

Table S1. Global cellular proteomic profiling of myoepithelial and luminal cell models

Table S2. Classification of cellular proteins based on myoepithelial, basal, and epithelial cell type

Table S3. Cohort numbers and correlation of myoepithelial or tumour stefin A staining (H-scores) to clinical features

25 Years ago in the *Journal of Pathology*...

Frequent expression of Epstein-Barr virus latent membrane protein-1 in tumour cells of Hodgkin's disease in HIV-positive patients

Dr Josée Audouin, Jacques Diebold and Gorm Pallesen

Herpes simplex virus type 1 DNA is present in specific regions of brain from aged people with and without senile dementia of the Alzheimer type

Gordon A. Jamieson, Norman J. Maitland, Gordon K. Wilcock, Celia M. Yates and Dr Ruth F. Itzhaki

To view these articles, and more, please visit:

www.thejournalofpathology.com

Click 'ALL ISSUES (1892 - 2017)', to read articles going right back to Volume 1, Issue 1.

The Journal of Pathology
Understanding Disease

